Blockchain Empowered Decentralized Storage in Air-to-Ground Industrial Networks

Yongxu Zhu, *Member, IEEE*, Gan Zheng, *Senior Member, IEEE*, Kai-Kit Wong, *Fellow, IEEE*

***Abstract*—Blockchain has created a revolution in digital networking, by using distributed storage, cryptographic algorithms, and smart contracts. Many areas are benefiting from this technology, including data integrity and security, as well as authentication and authorization. Internet of Things networks often suffers from such security issues, which is slowing down wide-scale adoption. In this paper, we describe employing blockchain technology to construct a decentralized platform for storing and trading information in the air-to-ground IoT heterogeneous network. To allow both air and ground sensors to participate in the decentralized network, we design a mutual-benefit consensus process to create uneven equilibrium distributions of resources among the participants. We use a Cournot model to optimize the active density factor set in the heterogeneous air network and then employ a Nash equilibrium to balance the number of ground sensors, which is influenced by the achievable average downlink rate between the air sensors and the ground supporters. Finally, we provide numerical results to demonstrate the beneficial properties of the proposed consensus process for air-to-ground networks and show the maximum active sensors density utilization of air networks to achieve a high quality of service.**

***Index Terms*—Blockchain, Industrial IoT, Stochastic Geometry, Cournot model, smart contract.**

I. Introduction

In the past ten years, blockchain technology has found extensive use in various fields beyond Bitcoin. The largest use of blockchain platforms is still in public ledgers for cryptocurrencies. However, there are increasing uses in non-financial applications. A recent trend is the use of blockchain technology to strengthen the data security and model the decentralized and consensus mechanism structures such as Internet of Things (IoT) applications using the next generation of wireless communication networking [1, 2].

Use of IoT technologies in various industries has attracted huge attention from both academics and governments [3]. Some IoT applications are developed closely with other industrial applications such as agriculture, environmental monitoring and security surveillance. The designers of industrial applications are, in particular, required to make an effort to find a good, sometimes subtle, balance between expense with benefits. [4] To address this challenge, blockchains Peer-to-Peer (P2P) approach could play an important role in the development of IoT decentralized systems and data intensive applications running on billions of devices, preserving the privacy of the users. This could apply in many circumstances, for example:

- *Public Health:* Fake medicine and food traceability are urgent problems in public health. For example, on a farm, a tamper-proof system to record growth data for crops and aquacultures could remove some sources of insecurity in supply chains.
- *Smart Cities:* Smart cities are using blockchain as the foundation of systems to monitor city parameters such as temperature, humidity and PM 2.5 levels. The best current example is Dubai [5], which aims to cement its status as a global leader in the smart economy by becoming the first blockchain-powered government.
- *Data storage management:* Blockchain-based distributed data storage clouds can be applied to health, justice, legislation, safety, and business systems, to protect sensitive sensor data, contracts, private data, etc.

A. Related Works

1) Blockchain Technology: Blockchain uses public-key cryptography to create a ledger for published transactions which is suitable for use in a *Peer-to-Peer* (P2P) network [6]. Once a new block has been saved into the blockchain, the transactions of that block will be confirmed [7]. To guarantee the integrity and consistency of the consensus protocol when updating the blockchain, one specific mining technique in Bitcoin network called *Proof-of-Work* (PoW) has been proposed. [7]. According to [8], PoW requires miners to spend their computational power on a computationally-hard puzzle, i.e., to find a partial preimage satisfying certain conditions of a hash mapping based on the proposed blockchain state. To solve the PoW puzzle, the author in paper [9] proposed an optimized solution which involved a cooperative computing offloading decision and content caching. The optimized result shows that the scheme could achieve better performance than that with deterministic constraints, and it could solve PoW puzzles more efficiently.

Another method uses the replaceable decentralized consensus protocols commonly used for Blockchain IoT networks, named *Proof-of-Stake* (PoS) [10]. In contrast to PoW, PoS demands much less CPU computation, energy, hardware, etc, in the mining process, and the opportunities for a node to mine the next block are related to the miners account to balance

Manuscript received October 15, 2018; revised December 18, 2019; accepted February 12, 2019. Part of this work was supported by the U.K. Engineering and Physical Sciences Research Council (EPSRC) under Grant EP/N007840/1 and EP/N008219/1. (*Corresponding author: Gan Zheng*)

Y. Zhu and G. Zheng are with the Wolfson School of Mechanical, Electrical and Manufacturing Engineering, Loughborough University, Leicestershire, LE11 3TU, UK (Email: {y.zhu4, g.zheng}@lboro.ac.uk).

K.-K. Wong is with the Department of Electronic and Electrical Engineering, University College London, London, WC1E 6BT, UK (Email: kai-kit.wong@ucl.ac.uk).

of stakes. The bigger the stake owned by a miner, the more mining power it has.

2) IoT blockchain: The central concept in IoT Blockchain is smart contracts, which allows the automation of complicated processes so that each participant benefits from and can trust such processes. The principles for applying blockchain technology to IoT network have been demonstrated [11]. The author points out that the purpose of sharing services and resources in decentralized IoT networks is to automate time-consuming workflows. In [12], the author describes a decentralized blockchain-based platform for data storage and trading in a wireless powered IoT crowd-sensing system. The data from RF-energy beacons are forwarded to the blockchain network for distributed ledger services, which provides the analytical condition for a range of valuable results about the equilibrium strategies in the blockchain-based network.

In paper [13], the author examined an optimization problem for edge computing resource management to analyse the interaction effect between the computing service provider and miners in the blockchain. A blockchain solution for the energy industry has been studied in [14, 15]. In [15], the author designed a credit-based payment method to solve the problem of confirmation delays in the transaction and intermittent connectivity of energy nodes. This blockchain solution can be applied to various IoT scenarios, such as energy harvesting networks and vehicle-to-grid. A P2P electricity trading model for Plug-in Hybrid Electric Vehicles (PHEVs) in smart grids was studied in paper [14]. That mechanism requires no third party when trading charging and discharging of PHEVs using the shared ledger. The authors conclude that this auction mechanism could enhance the security of transactions.

3) UAV-Based IoT Platforms: Providing real-time data is a significant function of UAVs, which could make images or videos of damaged nuclear reactors or other disasters. UAVs can connected to all kinds of IoT sensors and can be used to form a comprehensive P2P platform in the air [16].

A distributed trust system in an integrated unmanned aerial system was described in [17], whose ecosystem is made up of multi-tier partnerships, the human-robot trust between distributed entities. Paper [18] examined the secrecy performance of randomly deployed nodes to evaluate the UAV-enabled 3D antenna millimeter-wave based air-to-ground communication networks. However, for mechanical reasons, hovering UAVs suffer from high energy consumption; using traditional low-cost kites or balloons [19] could greatly reduce energy consumption, supporting more antennae or sending more information.

4) Data storage management: Data storage management is one of the most popular use cases of blockchain in IoT networks [20]. Combining blockchain and a P2P storage system to protect the sensitive data in IoT devices, data can be safely stored in different peers, and blockchain could guarantee their reliability and prevent tampering. A decentralized platform has been studied in [21], which protects personal private data using blockchain technology. Users of the platform can avoid the problem of the trustworthiness of any third party. It is also easy to collect and share sensitive data in legal and regulatory decisions. Paper [22] studies a decentralized cloud file storage platform named *Sia*, it uses cryptographic contracts to protect the storage agreements between clients and hosts. The host submits storage proofs to the network once a file is stored; the contracts are stored in a blockchain to provide a public audit.

5) Security: Blockchain depending on a distributed trust system could achieve high-security performance. However, blockchain technology still presents some potential security risks. For example, users in the system can suffer from the famous 51% attack that, anyone can forge the transaction if 51 % of the computation power is accumulated in one place. Anyone can leverage the computation power to intercept, modify and then rebroadcast the forged transaction where the system does not hold enough resource to validate.

The security of IoT systems is analysed in [23–25]. The author discusses a specific smart home system and proposes a blockchain-based framework to guarantee security, confidentiality, integrity, and availability. The security for information and energy interactions in the cloud as well as edge formed by electric vehicle nodes have been raised in [24]. Paper [25] proposed a secure P2P data sharing system in vehicular computing networks by utilising the concept of blockchain technologies Paper [26] investigates a Mobi-Chain which applies blockchain technology to a novel m-commerce application to protect the security of data. It concludes that blockchain technology is valid for future m-commerce security applications.

B. Contributions and Organization

Building on existing developments, we describe a novel mutual-benefit treaty in a blockchain-based heterogeneous cellular air-to-ground network. This model not only balances the interests of both heterogeneous air and ground networks but also protects data integrity under the consensus mechanism. This is in contrast to [22], which described a unilateral gain system whose benefits directly accrue to users. The advantage of decentralized storage air-to-ground networks is high-security performance, and they could achieve a closer connection link between two systems than the traditional centralized storage model. The main contributions of this paper are summarised as follows:

- We propose an innovative blockchain-based heterogeneous trading network. In the air-to-ground P2P jamming network, the Ground sensors (GS) allocate caching space to support Air sensors (AS) to secure the collected data. In return, the ASs send back certain rewards to the GS. This approach will significantly increase air data security and the ability to resist jamming signals. We develop a Quality-of-Service (QoS) optimization of the active ASs' output by designing a Cournot game model.
- Through this trading process, we propose a novel dual user-association strategy, the first user association aims to increase the average achievable rate, and the secondary user association not only balances the supply and demand in the air-to-ground market but also achieves the maximum benefit for both AS and GS networks.
- We explore two different reward allocation mechanisms in the P2P network, the numerical results demonstrate that

the group reward scheme (GRS) always achieves higher spectral efficiency than the individual reward scheme (IRS) in blockchain-empowered decentralized storage networks.

The rest of this paper is organized as follows. The system model is presented in Section II. The problem definition for trading contract for both the air and ground sides are provided in Section III. Simulation and numerical results, as well as discussions are given in Section V, followed by concluding remarks in Section VI.

II. System Model

We consider a heterogeneous air-to-ground blockchain-based decentralized network. In this system, ASs collect the data in the sky at different altitudes, then, because of the limited caching space and computation in the ASs, the active ASs broadcast the data to the ground network.

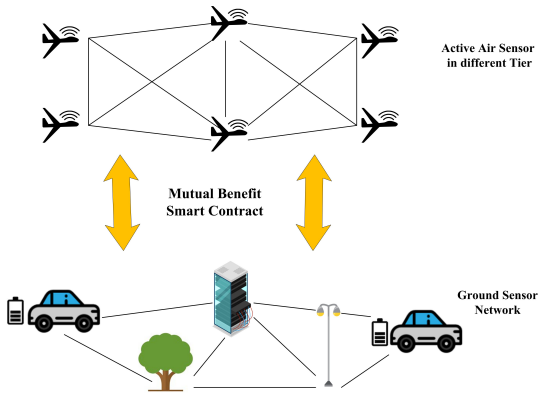

Fig. 1: Localized air-to-ground P2P Network. The GSs could equipped with smart grid vehicles, server, trees or street lamp.

In Fig. 2, all the sensors work in the air-to-ground network as trusted trading nodes with a smart contract. The GSs provide storage space for the active ASs according to their QoS function, then reward coins will be sent from the k-th tier ASs to the robust GSs. The locations of the GSs are modelled using a Homogeneous Poisson point process (HPPP) Φ_{G} with density λ_{G}. The locations of the ASs in the k-th tier ($k = 1, \cdots, K$) are modelled by an independent HPPP Φ_{A}^k with density λ_{A}^k. It is assumed that the density of GSs is much greater than ASs where $\lambda_{\mathrm{G}} > \sum_{k=1}^{K} \lambda_{\mathrm{A}}^k$, which can ensure that at least one GS could support the AS for the data storage process at each time slot T, the rest of ASs wait for the trading process in the following time slot. In the ASs set, the density declines with altitude, modelled by $\lambda_{\mathrm{G}} \gg \lambda_{\mathrm{A}}^1 > \cdots > \lambda_{\mathrm{A}}^k > \cdots > \lambda_{\mathrm{A}}^K$.

In addition, we call the active ASs who broadcast the collected data to the associated GSs in the present time slot in set $\widetilde{\Phi}_A^k \in \Phi_A^k$, where $\widetilde{\Phi}_A^k$ is the independent HPPP with density $a_k \lambda_A^k$. The remaining ASs buffer their data and wait to transmit in the next time slot, we refer to these as quiet ASs, which we model as having density $(1 - a_k)\lambda_A^k$ in set $\overline{\Phi}_A^k \in \Phi_A^k$, and we have $\widetilde{\Phi}_A^k + \overline{\Phi}_A^k = \Phi_A^k$, where $a_k \in [0, 1]$, which means the active ASs output decision affects the QoS for each tier of ASs.

More than that, the interpolators are not aware of which AS is generating new data until the transmission process starts. The ASs in different tiers have different susceptibility in the air environment, and the update data will be generated randomly by these sensors.

A. Consensus Process

The consensus process before transaction records forms the blockchain-based air-to-ground network as follows.

1) AS side–storage service requesting:

- Each tier of ASs in Φ_A^k generates a series of raw data sets from different altitudes. Then the active ASs who have generated data send requests to the contact centre. We assume that each active AS will request the service at the same time due to the massive information and information accuracy requirements.
- We define two types of incentive schemes. One is IRS, which means each active AS in the k-th tier will take out b_k coins for robust GS. The other scheme is GRS, in which all the GSs associated with the k-th tier UAVs will share the total reward of b_k^I coins.
- Based on the smart contract, each AS in a tier allocates the given reward 'coin' to prove their ability to finish payments for data storage.
- We establish a benefit function which aims for each tier of ASs to acquire maximum QoS in the trading market. Through the QoS function, the air network obtains the optimal active ASs set self-regulation via the reward of QoS in the market.

2) GS side–service support and coin payment:

- The typical GS $\mathcal{G}_o$ forecasts the achievable average rate for each tier of ASs based on the current optimized active density.
- Then the typical GS $\mathcal{G}_o$ does the secondary user association to decide the connection tier of AS, which aims to maximize the reward in unit time. The compensation depends on the units data reward 'coin' and the achievable average rate for each tier of ASs.
- The consensus protocol is implemented by authorized GSs and a robust GS $\mathcal{G}_L$ which connect to k-th tier AS and achieve maximum data in the given time slot with a valid PoS, note that the volume of data transferred depends on the available instantaneous data rate.
- Once all GSs agree on the block data and robust $\mathcal{G}_L$ get the reward coin, GS $\mathcal{G}_L$ is duty-bound to broadcast the block data and the corresponding signature to other GSs who did not participate in the competition for the same tier AS, which guarantees the block data security. Note that PoS is a protocol between a Prover and a Verifier [27] that has two phases.
- After that, the coin information is sent to GS $\mathcal{G}_L$. At the same time, the ASs update the coin information and release temporary storage space for the new information storage.
- In return, the ASs will help the coin owner GSs to collect the required information in the air, which could help GSs predict the weather or route in the future.

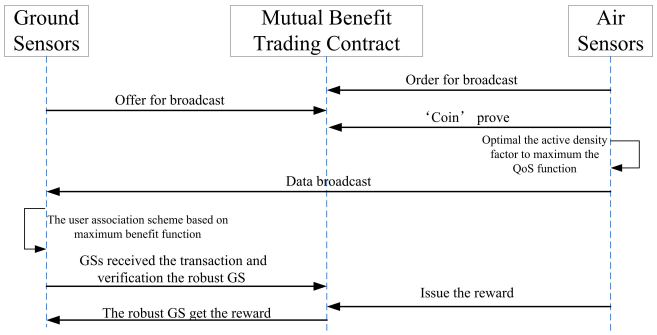

Fig. 2: Sequence diagram of the Air-to-Ground smart contract.

TABLE I: Notation and parameters.

Notation	Parameter
Φ_A^k, $\widetilde{\Phi}_A^k$, $\overline{\Phi}_A^k$	total AS PPP, active AS PPP and quite AS PPP
λ_A^k, a^k	AS density and active density factor
Φ_{G}, λ_{G}	GS PPP and density
Φ_e, λ_e	jamming PPP and density
T	duration time
$\mathbf{P}$, P_k	transmit power set and k-tier transmit power
$\mathbf{h}$, h_k	transmit power set and k-tier transmit power
α_{L}, α_{N}	LoS and NLoS path loss exponent
g	small scale fading
β, δ^2	the frequency dependent constant parameter, noise power

3) Blockchain Structure: In our blockchain-enabled air-to-ground system, blockchain technology is utilized to enhance the IoT block data secure performance from different IoT sensors. We use the IoT security blockchain-based framework [23] in our system, and each block incorporates a block header, a policy header and a group of block data.

B. Downlink Information Transfer

In the average rate predicted phase, AS transmits information signals to the serving GSs in the given duration time slot T with a specific transmit power power set $\mathbf{P} = [P_1, ..., P_k, ..., P_K]$, and the height set is $\mathbf{h} = [h_1, ..., h_k, ..., h_K]$ where $h_k < h_{k+1}$. Both ASs and GSs are equipped with a single antenna. We also consider the case of eavesdropping with jamming attacks to deteriorate the information transmission. The locations of eavesdroppers are modelled following an independent HPPP Φ_e with λ_e.

For a typical GS $\mathcal{G}_o$ associated with the AS who belongs to the given k-th tier. All channels experience independent identically distributed (i.i.d.) quasistatic Rayleigh fading. We assume that for any typical GS who is located at the point of origin o that is associated with the nearest AS in the k-th tier that has support to save the instant data, the received signal-to-interference-plus-noise ratio (SINR) is shown below:

$$\mathrm{SINR}_o^k = \frac{P_k g_{o,k} \beta |H_{o,k}|^{-\alpha_{\mathrm{L}}}}{\mathcal{I}_k^A + \mathcal{I}_K^J + \delta^2}, \tag{1}$$

where P_k is the transmit power for the k-th tier AS, $g_{o,k}$ is the equivalent small-scale fading channel power gain between the typical GS $\mathcal{G}_o$ and its nearest serving k-th tier AS. Notice when $\mathcal{G}_o$ is associated to K-th tier, the path loss is $|H_{o,k}|^{-\alpha_{\mathrm{L}}}$, where $H_{o,k} = \sqrt{{X_{o,k}}^2 + h_k^2}$ is the distance from the associated AS to the typical GS, β is the frequency dependent constant parameter and α_{L} is the line of sight (LoS) path loss exponent. Due to building blockages in the terrestrial environment, the direct connection between GSs is weak. We consider the LoS link and same path loss exponent α_{L} between different tier of ASs to GSs, and the non-line-of-sight (NLoS) link between GSs [28]. δ^2 is the noise power.

The interference $\mathcal{I}_k^A$ from the all the active ASs from k-th tier and other tiers which are given by

$$\mathcal{I}_k^A = \sum_{k'=1\backslash k}^{K} \sum_{l \in \widetilde{\Phi}_A^{k'}} P_{k'} g_{o,k'} \beta |H_{o,k'}|^{-\alpha_{\mathrm{L}}} \tag{2a}$$

$$+ \sum_{j \in \widetilde{\Phi}_A^k \backslash o} P_k g_{o,j} \beta |H_{o,j}|^{-\alpha_{\mathrm{L}}}. \tag{2b}$$

(2a) and (2b) are the sum of interference from the interfering ASs in the k'-tier ($k' \neq k$) and the k-tier, $\Phi_A^{k'}$ and Φ_A^k are the point process with density $\lambda_A^{k'}$ and λ_A^k, where $g_{o,l} \sim \exp(1,1)$ and $g_{o,k} \sim \exp(1,1)$ are the small-scale fading interfering channel gain and $H_{o,k'} = \sqrt{{X_{o,k'}}^2 + h_{k'}^2}$ is the distance between a typical GS and the k'-th tier AS $l \in \widetilde{\Phi}_A^{k'}$. The channel is authenticated to prevents eavesdropper from tampering with the messages. We assume that all the eavesdroppers transmit jamming signals to the GS, and $\mathcal{I}^J(k)$ is the interference from the jamming which is give by

$$\mathcal{I}_k^J = \sum_{e \in \Phi_e} P_e g_{o,e} \beta |X_{o,e}|^{-\alpha_{\mathrm{N}}}, \tag{3}$$

where Φ_e is the locations of the ground eavesdroppers with density λ_e, where $g_{o,e} \sim \exp(1)$ is the small-scale fading interfering channel gain and $X_{o,e}$ is the distance between the $\mathcal{G}_o$ and ground eavesdropper, and α_{N} is the none line of sight (NLoS) path loss exponent.

III. Problem Definition for Trading Contract

In this section, we present the trading process which includes the optimized QoS function for each tier of AS, and then we figure out the probability that a typical GS is associated with the AS in the k-th tier based on the achievable average k-th tier rate.

In the trading process, each AS buffers data, which must be transmitted as soon as possible, due to the limited storage space in the ASs and high demand for effective security. The AS generates the updated data then asks GS to help store the data and prevent the information being tampered with. Each GS will take out a certain amount of coin for reward, but only the most robust GS named $\mathcal{G}_{\mathrm{L}}$ will get the reward. In the future, the robust GS $\mathcal{G}_{\mathrm{L}}$ could use the reward 'coin' to request service for the air group to do the data ferry from more distant nodes.

A. The Cournot-Nash equilibrium In Air Side

For the air side, each tier of AS will compete to attract more GSs to support the data storage. However, the more active that ASs are in the trading market, the less associated service GSs there will be for each AS at any given time.

We assume the exact achievable rate for each tier is unknown where each UAV has incomplete information on other tiers of UAVs parameters, such as the height set **h** and the transmit power set **P**. The convergence to the Nash equilibrium in such a market is then analysed using the well-known best response dynamics.

Based on that, we use the **Cournot-Nash equilibrium** to model the QoS function. The AS in k-th tier form a consensus group which expect maximized profits, and their own active density decisions will affect the results of their rivals (k'-tier of AS).The profit maximization problem of the IRS is simplified as follows:

$$\mathbb{P}_1 \quad \max_{\mathbf{a}^{(1)}} \quad \mathrm{Q}_k^{(1)} = a_k^{(1)} \lambda_A^k (\rho_I - b_k), \tag{4a}$$

$$\text{s.t.} \quad \mathrm{C1}: \rho_I = -\theta_1 \mathcal{N}_A + \theta_0, \tag{4b}$$

$$\mathrm{C2}: 0 \leq a_k \leq 1, \tag{4c}$$

where in (4a), Q_k is the total QoS function in the k-tier, which means a high value could provide more support to the k-th tier AS. We assume that all the ASs in k-th consensus tier are given the same QoS reward because they collect the same type of data in the air. Each tier of AS chooses its optimal active factor a_k independently, and the whole system determines how to achieve the benefit equilibrium for every participant.

Notice that in this process, we assume that information ρ_k is only imperfectly known by different tier rivals, so the QoS function assumes ρ_I denotes the equilibrium service of storage by the competition among the ASs, and ρ_k is supposed to be equal here.

The inverse demand function in (4b), $\rho_I = -\theta_1 \mathcal{N}_A + \theta_0$ is subject to $\frac{d\rho_I}{d\mathcal{N}_A} < 0$, and the equilibrium is always inverse ratio with the number of request group $\mathcal{N}_A$, where $\mathcal{N}_A = \mathcal{A}_u \sum_{k=1}^{K} a_k \lambda_A^k$ is the total active density in the unit area market $\mathcal{A}_u$, θ_0 and θ_1 are the positive constant coefficients.

Because λ_k is fixed, we adjust a_k to decide how much data an active AS broadcasts in each slot and achieve the maximum QoS function Q_k, and the range for the active proportion is $a_k \in [0, 1]$. Notice although the QoS function $\mathrm{Q}_k^{(1)}$ is based on imperfect information, and it could not predict the practical QoS for each tier, however, before the GS makes the final decision, AS could control the broadcast group to achieve the approximate optimal QoS.

Lemma 1: The optimal active density factor set $\mathbf{a}_k$ in problem $\mathbb{P}_1$ can be expressed as follows

$$\mathbf{a}^{(1)^*} = [a_1^{(1)^*}, a_2^{(1)^*}, ..., a_K^{(1)^*}] \tag{5}$$

where $a_k^{(1)^*} = \max\left[\min\left[\frac{1}{\theta_1 \lambda_A^k}\left(\frac{\theta_0 + \sum_{k=1}^{K} b_k}{K+1} - b_k\right), 1\right], 0\right]$ is the active proportion for density of the k-th AS.

Proof 1: Substitute $\rho_I = -\theta_1 \mathcal{N}_A^{(1)} + \theta_0$ into $\mathrm{Q}_k^{(1)}$, it can be expressed as:

$$\begin{aligned} \mathrm{Q}_k^{(1)} &= a_k^{(1)} \lambda_A^k (\theta_0 - \theta_1 \mathcal{A}_u \sum_{k=1}^{K} a_k^{(1)} \lambda_A^k - b_k) \\ &= -\theta_1 \left(a_k^{(1)} \lambda_A^k\right)^2 + a_k^{(1)} \lambda_A^k (\theta_0 - \theta_1 \mathcal{A}_u \sum_{k'=1\backslash k}^{K} a_{k'}^{(1)} \lambda_A^{k'} - b_k), \end{aligned} \tag{6}$$

the first derivative equation can be expressed as:

$$\begin{aligned} &\frac{d\mathrm{Q}_k^{(1)}}{da_k^{(1)}} \\ &= -2\theta_1 a_k^{(1)} \left(\lambda_A^k\right)^2 + \lambda_A^k (\theta_0 - \theta_1 \mathcal{A}_u \sum_{k'=1\backslash k}^{K} a_{k'}^{(1)} \lambda_A^{k'} - b_k). \end{aligned} \tag{7}$$

From (14), $\mathrm{Q}_k^{(1)}$ is the continuous quadratic function of $a_k^{(1)}$, and the second derivative of $\mathrm{Q}_k^{(1)}$ with the respect to $a_k^{(1)}$ is

$$\frac{d^2 \mathrm{Q}_k^{(1)}}{{da_k^{(1)}}^2} = -2\theta \left(\lambda_A^k\right)^2 < 0, \tag{8}$$

then we can obtain that $\mathrm{Q}_k^{(1)}$ is a concave function of $a_k^{(1)}$. Therefore, we can obtain the optimal output of $\mathrm{Q}_k^{(1)}$ by setting the first derivative equal (14) to zero, then obtain $a_k^{(1)}$ as

$$a_k^{(1)} = -\frac{\mathcal{A}_u}{2\lambda_A^k} \sum_{k'=1\backslash k}^{K} a_{k'}^{(1)} \lambda_A^{k'} + \frac{\theta_0 - b_k}{2\theta_1 \lambda_A^k}. \tag{9}$$

We can figure out the total active number of UAVs at one slot as follows:

$$\mathcal{N}_A^{(1)^*} = \max\left[\min\left[\frac{K\theta_0 - \sum_{k=1}^{K} b_k}{\theta_1 (K+1)}, \mathcal{A}_u \sum_{k=1}^{K} \lambda_A^k\right], 0\right], \tag{10}$$

after that, we can obtain the optimal a_k with (15) and (16) as follow

$$a_k^{(1)^{op}} = \frac{1}{\theta_1 \lambda_A^k}\left(\frac{\theta_0 + \sum_{k=1}^{K} b_k}{K+1} - b_k\right), \tag{11}$$

based on $a_k^{(1)^*} = \max\left[\min\left[a_k^{(1)^{op}}, 1\right], 0\right]$, we completes the proof.

Given that each k-th tier of UAV has been assigned with b_k^I coin, then we can deduce the profit maximization of the GRS as follows

$$\mathbb{P}_2 \quad \max_{\mathbf{a}^{(2)}} \quad \mathrm{Q}_k^{(2)} = a_k^{(2)} \lambda_A^k (\rho_I - \frac{b_k^I}{a_k^{(2)} \lambda_A^k}), \tag{12a}$$

$$\text{s.t.} \quad \mathrm{C1}: \rho_I = -\theta_1 \mathcal{N}_A^{(2)} + \theta_0, \tag{12b}$$

$$\mathrm{C2}: 0 \leq a_k^{(2)} \leq 1, \tag{12c}$$

Lemma 2: The optimal active density factor set $\mathbf{a}_k$ for maximum the problem $\mathbb{P}_2$ can be expressed as follows

$$\mathbf{a}^{(2)^*} = [a_1^{(2)^*}, a_2^{(2)^*}, ..., a_K^{(2)^*}], \tag{13}$$

where $a_k^{(2)^*} = \max\left[\min\left[\frac{1}{\lambda_A^k}\left(\frac{\theta_0}{\theta_1} - \frac{K}{K+1}\right), 1\right], 0\right]$.

Proof 2:

Similar with $\mathbb{P}_1$, we desired the first derivative equation for $\mathrm{Q}_k^{(2)}$ can be expressed as:

$$\frac{d\mathrm{Q}_k^{(2)}}{da_k^{(2)}} = -2\theta a_k^{(2)} \left(\lambda_A^k\right)^2 + \lambda_A^k (\theta_0 - \sum_{k'=1\backslash k}^{K} \theta_1 a_{k'}^{(2)} \lambda_A^{k'}). \tag{14}$$

Then we derive that $\mathrm{Q}_k^{(2)}$ is a concave continuous quadratic function of $a_k^{(2)}$, due to the second derivative of $\frac{d^2 \mathrm{Q}_k}{{da_k}^2} < 0$.

Therefore, we can obtain the optimal output of $\frac{d\mathrm{Q}_k^{(2)}}{da_k^{(2)}}=0$ to obtain $a_k^{(2)}$ as

$$a_k^{(2)}=\frac{\theta_0-\theta_1\sum_{k'=1\backslash k}^{K}a_{k'}^{(2)}\lambda_A^{k'}}{2\theta_1\lambda_A^k}, \tag{15}$$

Substituting the optimal value in (15), we have the total active number of UAVs at one slot as follows:

$$\mathcal{N}_A^{(2)^*}=\max\left[\min\left[\frac{K\theta_0}{\theta_1\left(K+1\right)},\sum\nolimits_{k=1}^{K}\lambda_A^k\right],0\right], \tag{16}$$

after that, we can obtain the optimal a_k with (15) and (16) as follow

$$a_k^{(2)^{op}}=\frac{1}{\lambda_A^k}\left\{\frac{\theta_0}{\theta_1}-\frac{K}{K+1}\right\}, \tag{17}$$

based on $a_k^{(2)^*}=\max\left[\min\left[a_k^{(2)^{op}},1\right],0\right]$, then we completes the proof.

B. Downlink Performance Evaluation In GS side

Before broadcasting the data, the typical GS $\mathcal{G}_o$ figures out the achievable rate with each tier of AS with given active proportion. Once typical GS $\mathcal{G}_o$ selects the given kth-tier AS, it will be associated to the closest AS according to data storage requirements, the connect probability for the k-tier is $f_k(x)=2\pi a_k\lambda_k x e^{-x^2\pi a_k\lambda_k}$.

***Lemma** 3:* The achievable average downlink achievable rate between a typical GS $\mathcal{G}_o$ and its serving the nearest AS in k-th tier is as follows:

$$\mathcal{R}_k(\mathbf{a}^*)=\frac{1}{\ln 2}\int_0^\infty\int_0^\infty\frac{\mathcal{P}_k^{\mathrm{cov}}(x,\gamma_o)}{1+\gamma_o}f_k\left(x\right)dxd\gamma_o \tag{18}$$

where $\mathcal{P}_k^{\mathrm{cov}}(x,\gamma_o)$ is given in (19) shown at the top of the next page. The constant $\chi_{\mathrm{N}}=\frac{2}{\alpha_{\mathrm{N}}}$, $\chi_{\mathrm{L}}=\frac{\alpha_{\mathrm{L}}}{2}$, $\csc(\cdot)$ is the cosecant-trigonometry function. For ease of notation, we define the following two functions O_k and $\mathrm{O}_{k'}$, which are related to the interference from the AS s in the k-th tier and other tiers, respectively:

$$\mathrm{O}_k(x,\gamma_o)=\int_{\sqrt{{h_k}^2+x^2}}^\infty\frac{1}{\left(\frac{r^2+h_k^2}{x^2+h_k^2}\right)^{\chi_{\mathrm{L}}}/\gamma_o+1}rdr, \tag{20}$$

$$\mathrm{O}_{k'}(x,\gamma_o)=\int_{h_{k'}}^\infty\frac{1}{P_k\left(\frac{r^2+h_{k'}^2}{x^2+h_k^2}\right)^{\chi_{\mathrm{L}}}/\left(\gamma_o P_{k'}\right)+1}rdr. \tag{21}$$

***Proof** 3:* The outage coverage probability is as follows

$$\mathcal{P}_k^{\mathrm{cov}}(x,\gamma_o)=\Pr\left(\mathrm{SINR}_{o,i}(k)\geqslant\gamma_o\right), \tag{22}$$

where $\mathcal{P}_k^{\mathrm{cov}}(x,\gamma_o)$ is the CCDF of the received SINR from typical GS to the associated AS, denoted by SINR_o^k, and is given by

$$\begin{aligned}\mathcal{P}_k^{\mathrm{cov}}(x,\gamma_o)&=\Pr\left(\frac{P_k g_{o,k}\beta\left(x^2+{h_k}^2\right)^{-\frac{\alpha_{\mathrm{L}}}{2}}}{\mathcal{I}_k^A+\mathcal{I}_k^J+\delta^2}>\gamma_o\right)\\&=e^{-\frac{\delta^2\left(x^2+h_k^2\right)^{\frac{\alpha_{\mathrm{L}}}{2}}\gamma_o}{P_k\beta}}\\&\mathbb{E}\left\{e^{-\frac{\mathcal{I}^A\delta^2\left(x^2+h_k^2\right)^{\frac{\alpha_{\mathrm{L}}}{2}}\gamma_o}{P_k\beta}}\right\}\mathbb{E}\left\{e^{-\frac{\mathcal{I}^J\delta^2\left(x^2+h_k^2\right)^{\frac{\alpha_{\mathrm{L}}}{2}}\gamma_o}{P_k\beta}}\right\}\\&=e^{-\frac{\delta^2\left(x^2+h_k^2\right)^{\frac{\alpha_{\mathrm{L}}}{2}}\gamma_o}{P_k\beta}}\mathcal{L}_{\mathcal{I}^A}\left(s_k\right)\mathcal{L}_{\mathcal{I}^J}\left(s_k\right),\end{aligned} \tag{23}$$

where $s_k=\frac{\left(x^2+h_k^2\right)^{\frac{\alpha_{\mathrm{L}}}{2}}\gamma_o}{P_k\beta}$, and $\mathcal{L}_{\mathcal{I}^A}\left(s_k\right)$ and $\mathcal{L}_{\mathcal{I}^J}\left(s_k\right)$ are the Laplace transforms of the PDFs of $\mathcal{I}^A$ and $\mathcal{I}^J$. By applying the stochastic geometry, we derive the Laplace transform of the PDF of $\mathcal{I}^A$:

$$\begin{aligned}\mathcal{L}_{\mathcal{I}^A}(s)&=\mathbb{E}_{\Phi_k^A}\left[\exp\left(-s_k\sum_{i\in\widetilde{\Phi}_k^A}P_k h_{o,i}\beta{H_{o,i}}^{\alpha_{\mathrm{L}}}\right)\right]\\&+\mathbb{E}\left\{\sum_{k'=1\backslash\{k\}}^{K}\exp\left(-s_k\sum_{l\in\widetilde{\Phi}_{k'}^A}P_{k'}h_{o,l}\beta{H_{o,l}}^{\alpha_{\mathrm{L}}}\right)\right\}\\&=\exp\left\{-2\pi a_k\lambda_k\times\right.\\&\left.\int_{\sqrt{{h_k}^2+x^2}}^\infty\left(1-\frac{1}{1+s_kP_k\beta(r^2+h_k^2)^{-\chi_{\mathrm{L}}}}\right)rdr\right\}\\&\times\prod_{k'=1\backslash\{k\}}^{K}\exp\left\{-2\pi a_{k'}\lambda_{k'}\times\right.\\&\left.\int_{h_{k'}}^\infty\left(1-\frac{1}{1+s_kP_{k'}\beta(r^2+h_{k'}^2)^{-\chi_{\mathrm{L}}}}\right)rdr\right\}.\end{aligned} \tag{24}$$

Using a similar approach in (24), we derive the interference coming from the jamming signal as follows

$$\begin{aligned}\mathcal{L}_{\mathcal{I}^J}(s_k)&=\mathbb{E}_{\Phi^J}\left[\exp\left(-s_k\sum_{j\in\Phi^J}P_e h_{o,e}\beta{y_{o,e}}^{\alpha_{\mathrm{N}}}\right)\right]\\&\overset{(a)}{=}\exp\left[-2\pi\lambda_e\int_0^\infty\left(1-\frac{1}{1+s_kP_e\beta{r_e}^{-\alpha_{\mathrm{N}}}}\right)r_e dr_e\right],\end{aligned} \tag{25}$$

where (a) is obtained by using the generating functional of PPP [29]. After that, we can obtain (24) and (25) of the SINR in (23), and this completes the proof.

Based on the predicted average achievable rate $\mathcal{R}_k(\mathbf{a}^{(1)^*})$ which is associated to a k-th tier AS, we can build the secondary user association scheme, which aims to maximize the benefit for the typical GS. The serving AS for a typical GS based on the IRS $\mathbb{P}_1$ is selected according to the following criterion:

$$\mathrm{GS}:\arg\max_{k\in1,2,\ldots,K}{\mathcal{F}_k}^*, \tag{26}$$

$$\mathcal{P}_k^{\mathrm{cov}}(\gamma_o) \tag{19}$$
$$= \exp\left\{-\frac{\delta^2\gamma_o}{P_k\beta}\left(x^2+h_k^2\right)^{\chi_{\mathrm{L}}} - \lambda_e\chi_{\mathrm{N}}\pi\csc\left(\chi_{\mathrm{N}}\pi\right)\left(x^2+h_k^2\right)^{\chi_{\mathrm{N}}\chi_{\mathrm{L}}}\left(\frac{\gamma_o P_e}{P_k}\right)^{\chi_{\mathrm{N}}} - 2\pi a_k\lambda_k \mathrm{O}_k - 2\pi\sum_{k'=1\setminus\{k\}}^{K} a_{k'}\lambda_{k'}\mathrm{O}_{k'}\right\}$$

where

$$\mathcal{F}_k{}^* = \mathcal{R}_k(\mathbf{a}^{(1)^*})\cdot b_k\cdot\Psi_k^{(1)}, \tag{27}$$

since each typical GS is only associated to one UAV, and $\Psi_k^{(1)}$ is the success probability that the typical GS turns into the robust GS and obtains the reward b_k. Notice that even though only a proportion of GSs support the k-th tier ASs at each slot, the block data will be copied to all the other GSs in the P2P network. Then we can see this is a Nash Equilibrium problem in which the typical GS will reward the equal benefit $\mathcal{F}$ from any tier of AS. Then we can formulate the secondary user association probability for the IRS $\mathbb{P}_1$ expression as:

$$\Psi_k^{(1)^*} = \frac{1}{\mathcal{R}_k(\mathbf{a}^{(1)^*})b_k}\frac{1}{\sum_{k=1}^{K}\frac{1}{\mathcal{R}_k(\mathbf{a}^{(1)^*})b_k}}. \tag{28}$$

Overall, for a typical GS in the heterogeneous UAV network with dual user association, the average achievable rate can be calculated as

$$\mathcal{R}_{\mathrm{HetNet}}^{(1)} = \sum_{k=1}^{K}\Psi_k^{(1)}\mathcal{R}_k(\mathbf{a}^{(1)^*}). \tag{29}$$

For the $\mathbb{P}_2$ bonus scheme, the secondary user association for the serving AS for a typical GS is selected according to the following criterion:

$$\mathrm{GS}: \arg\max_{k\in 1,2,\ldots,K}\mathcal{R}_k(\mathbf{a}^{(2)^*})\cdot\frac{b_k}{a^{(2)^*}\lambda_k}, \tag{30}$$

where

$$\mathcal{F}_k{}^* = \mathcal{R}_k(\mathbf{a}^{(2)^*})\cdot\frac{b_k}{a^{(2)^*}\lambda_k}\cdot\Psi_k^{(2)}, \tag{31}$$

the secondary user association probability for bonus scheme $\mathbb{P}_2$ expression as:

$$\Psi_k^{(2)^*} = \frac{a_k^{(2)*}\lambda_k^A}{\mathcal{R}_k(\mathbf{a}^{(2)^*})b_k^I}\frac{1}{\sum_{k=1}^{K}\frac{a_k^{(2)*}\lambda_k^A}{\mathcal{R}_k(\mathbf{a}^{(2)^*})b_k^I}}. \tag{32}$$

Then we can obtain the average achievable rate for a typical GS in the heterogeneous UAV network with dual user association as

$$\mathcal{R}_{\mathrm{HetNet}}^{(2)} = \sum_{k=1}^{K}\Psi_k^{(2)}\mathcal{R}_k(\mathbf{a}^{(2)^*}). \tag{33}$$

IV. Numerical Results

In this section, we present the numerical results to examine the impact of the reward functions on both the GS and AS network. We consider an air-to-ground blockchain-based hybrid network, with six different tiers in the air system.

All the parameters used in the simulation are carefully selected and well referenced. The transmit power of different tier of ASs are $\mathbf{P} = [20, 20, 23, 23, 30, 30]$ dBm, given the mobile-to-tower output power listed in the 3GPP channel model [30]. Also, considering the frequency requirement used in aircraft, we have $f_c = 2.43$ GHz. The path loss exponent in urban micro-cellular for LoS and NLoS are α_{L}=2 and α_{N}=3.1, respectively [31]. And finally, we design the heterogeneous ASs system to work on an altitude lower than 27 kilometres for information interaction and collection [32].

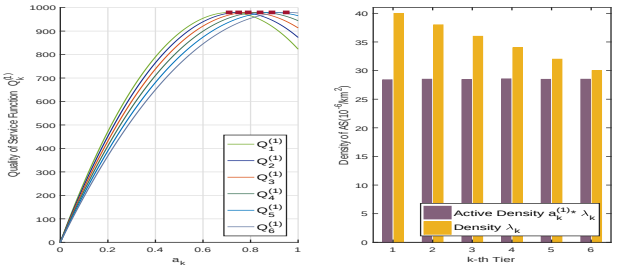

(a) Individual reward scheme (IRS).

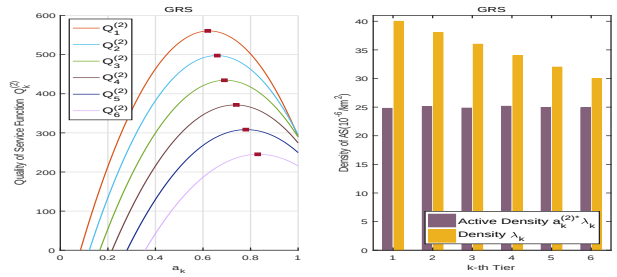

(b) Group reward scheme (GRS).

Fig. 3: The optimal active density $a_k\lambda_k^A$ and total density λ_k^A in different tier and the utility of QoS function $\mathrm{Q_k}$ in different tiers against active density factor a_k.

In the Fig. 3 we evaluate the optimal density in each tier in (5) for IRS and (13) for GRS which compare with the original total density set $\lambda^A = [40, 38, 36, 34, 32, 30]$/km^2. We have constant $\theta_1 = 1.2\times10^{11}$ and $\theta_0 = 6\times10^7$, the unit area is $\mathcal{A}_u = 1$. We assume the reward 'coin' for IRS as $\mathbf{b} = [3, 4, 5, 6, 7, 8]\times10^2$, and the reward 'coin' for GRS as $\mathbf{b}^I = [3, 4, 5, 6, 7, 8]\times10^{1.8}$. Firstly, we observe that an optimal active density factor exists for both schemes to obtain the maximum QoS function $\mathrm{Q_k}$. The optimal set $\mathbf{a}^*$ are $\mathbf{a}^{(1)^*} = [0.71, 0.75, 0.79, 0.84, 0.89, 0.95]$ and $\mathbf{a}^{(2)^*} = [0.62, 0.66, 0.69, 0.74, 0.78, 0.83]$ factor, marked with red squares from tier 1 to 6, respectively. We also observe that in both of these two schemes, the optimal active densities generally have similar values. In Fig. 3(a), we observe that the optimal $\mathrm{Q_k^{(1)}}$ is almost at the same level on each tier, but the optimal $\mathrm{Q_k^{(2)}}$ in Fig. 3(b) decreases from tier one to tier six. This is because in this trading market, even the upper tier with low density, but it keeps a higher active density to guarantee the balance of the trading market.

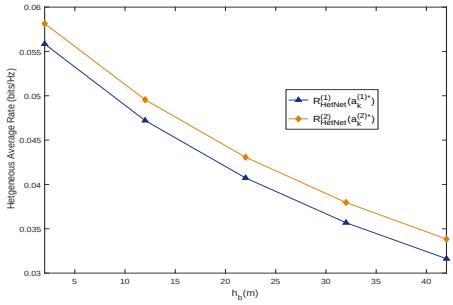

Fig. 4: Average heterogeneous rate via different height

Fig. 4 shows the impact of the AS height set on the average heterogeneous achievable rates. In order to better analyse the average rate performance, we assume a minimum height h_b and the actual height set is $\mathbf{h} = h_b + [20, 22, 24, 26, 28, 30]$ m. The analytical curves show (29) and (33) for IRS and GRS, respectively. We observe that the $\mathcal{R}^{(2)}_{\text{HetNet}}$ is always better than $\mathcal{R}^{(1)}_{\text{HetNet}}$, and GRS pay lower reward 'coin' than IRS. The result shows that dynamic allocation reward resource is more economical and achieve a higher performance for the heterogeneous decentralized network.

V. Conclusion

In this paper, we proposed a blockchain-based air to ground communication system that embraced the concepts of distributed data storage and mutually beneficial transactions, to enable secure and efficient information transmission in industrial IoT networks. While the security issues in data storage and transmission become more and more critical in IoT networks, the decentralized network can protect data integrity, as well as building up an eco-system among the heterogeneous networks. The simulation results show that the trading consensus process can be usefully adopted in the air-to-ground industrial IoT system, the optimized active density could maximize the QoS for AS and increase the transmission rate for the information exchange system.

References

[1] N. Kshetri, "Can blockchain strengthen the Internet of Things?" *IT Professional*, vol. 19, no. 4, pp. 68–72, Aug. 2017.

[2] S. M. Z. C. Q. H. Y. Dai, D. Xu and Y. Zhang, "Blockchain and deep reinforcement learning empowered intelligent 5G beyond," *IEEE Network Mag.*, pp. 1–1, Jan. 2019.

[3] Y. Li, M. Hou, H. Liu, and Y. Liu, "Towards a theoretical framework of strategic decision, supporting capability and information sharing under the context of internet of things," *Information Technology and Management*, vol. 13, no. 4, pp. 205–216, 2012.

[4] L. D. Xu, W. He, and S. Li, "Internet of things in industries: A survey," *IEEE Trans. Ind. Infor.*, vol. 10, no. 4, pp. 2233–2243, Nov. 2014.

[5] N. Lohade, "Dubai aims to be a city built on blockchain," *Wall Street Journal*, 2017.

[6] S. Nakamoto, "Bitcoin: A peer-to-peer electronic cash system."

[7] M. Conoscenti, A. Vetr, and J. C. D. Martin, "Blockchain for the Internet of Things: A systematic literature review," in *2016 IEEE/ACS 13th International Conference of Computer Systems and Applications (AICCSA)*, Agadir, Morocco, Nov. 2016, pp. 1–6.

[8] J. Garay, A. Kiayias, and N. Leonardos, "The bitcoin backbone protocol: Analysis and applications," in *Annual International Conference on the Theory and Applications of Cryptographic Techniques*. Springer, 2015, pp. 281–310.

[9] M. Liu, F. R. Yu, Y. Teng, V. C. M. Leung, and M. Song, "Computation offloading and content caching in wireless blockchain networks with mobile edge computing," *IEEE Trans. Veh. Technol.*, vol. 67, no. 11, pp. 11 008–11 021, Nov. 2018.

[10] K. Yeow, A. Gani, R. W. Ahmad, J. J. P. C. Rodrigues, and K. Ko, "Decentralized consensus for edge-centric internet of things: A review, taxonomy, and research issues," *IEEE Access*, vol. 6, pp. 1513–1524, 2018.

[11] K. Christidis and M. Devetsikiotis, "Blockchains and smart contracts for the internet of things," *IEEE Access*, vol. 4, pp. 2292–2303, May 2016.

[12] S. Feng, W. Wang, D. Niyato, D. I. Kim, and P. Wang, "Competitive data trading in wireless-powered internet of things (IoT) crowdsensing systems with blockchain," *arXiv preprint arXiv:1808.10217*, 2018.

[13] Z. Xiong, S. Feng, D. Niyato, P. Wang, and Z. Han, "Optimal pricing-based edge computing resource management in mobile blockchain," in *2018 IEEE International Conference on Communications (ICC)*, May 2018, pp. 1–6.

[14] J. Kang, R. Yu, X. Huang, S. Maharjan, Y. Zhang, and E. Hossain, "Enabling localized peer-to-peer electricity trading among plug-in hybrid electric vehicles using consortium blockchains," *IEEE Trans. Ind. Infor.*, vol. 13, no. 6, pp. 3154–3164, Dec. 2017.

[15] Z. Li, J. Kang, R. Yu, D. Ye, Q. Deng, and Y. Zhang, "Consortium blockchain for secure energy trading in industrial internet of things," *IEEE Trans. Ind. Infor.*, vol. 14, no. 8, pp. 3690–3700, Aug. 2018.

[16] N. H. Motlagh, M. Bagaa, and T. Taleb, "UAV-based IoT platform: A crowd surveillance use case," *IEEE Commun. Mag.*, vol. 55, no. 2, pp. 128–134, Feb. 2017.

[17] K. E. Oleson, P. Hancock, D. R. Billings, and C. D. Schesser, "Trust in unmanned aerial systems: A synthetic, distributed trust model," in *GPaper presented at the 16th International Symposium on Aviation Psychology*, Dayton, OH, 2011.

[18] Y. Zhu, G. Zheng, and M. Fitch, "Secrecy rate analysis of UAV-enabled mmwave networks Using Matérn hardcore point processes," *IEEE J. Sel. Areas Commun.*, vol. 36, no. 7, pp. 1397–1409, July 2018.

[19] F. Nex and F. Remondino, "UAV for 3D mapping applications: a review," *Applied geomatics*, vol. 6, no. 1, pp. 1–15, Mar. 2014.

[20] M. Conoscenti, A. Vetr, and J. C. D. Martin, "Blockchain for the internet of things: A systematic literature review," in *2016 IEEE/ACS 13th International Conference of Computer Systems and Applications (AICCSA)*, Nov. 2016, pp. 1–6.

[21] G. Zyskind, O. Nathan, and A. Pentland, "Decentralizing privacy: Using blockchain to protect personal data," in *2015 IEEE Security and Privacy Workshops*, May 2015, pp. 180–184.

[22] D. Vorick and L. Champine, "Sia: Simple decentralized storage," 2014.

[23] A. Dorri, S. S. Kanhere, R. Jurdak, and P. Gauravaram, "Blockchain for IoT security and privacy: The case study of a smart home," in *IEEE International Conference on Pervasive Computing and Communications Workshops (PerCom Workshops)*, Mar. 2017, pp. 618–623.

[24] H. Liu, Y. Zhang, and T. Yang, "Blockchain-enabled security in electric vehicles cloud and edge computing," *IEEE Network*, vol. 32, no. 3, pp. 78–83, May 2018.

[25] J. Kang, R. Yu, X. Huang, M. Wu, S. Maharjan, S. Xie, and Y. Zhang, "Blockchain for secure and efficient data sharing in vehicular edge computing and networks," *IEEE J. Inter. of Thi.*, pp. 1–1, 2019.

[26] K. Suankaewmanee, D. T. Hoang, D. Niyato, S. Sawadsitang, P. Wang, and Z. Han, "Performance analysis and application of mobile blockchain," in *2018 International Conference on Computing, Networking and Communications (ICNC)*, Mar. 2018, pp. 642–646.

[27] S. Park, K. Pietrzak, J. Alwen, G. Fuchsbauer, and P. Gazi, "Spacecoin: A cryptocurrency based on proofs of space," IACR Cryptology ePrint Archive, Tech. Rep., 2015.

[28] T. Riihonen, S. Werner, and R. Wichman, "Hybrid full-duplex/half-duplex relaying with transmit power adaptation," *IEEE Trans. Wireless Commun.*, vol. 10, no. 9, pp. 3074–3085, Sep. 2011.

[29] M. Haenggi, *Stochastic Geometry for Wireless Networks*. Cambridge University Press, 2013.

[30] 3GPP TR 36.814, "Further advancements for E-UTRA physical layer aspects (V9.0.0)", Mar. 2010.

[31] S. Sun, T. S. Rappaport, S. Rangan, T. A. Thomas, A. Ghosh, I. Z. Kovacs, I. Rodriguez, O. Koymen, A. Partyka, and J. Jarvelainen, "Propagation path loss models for 5g urban micro- and macro-cellular scenarios," in *Vehicular Technology Conference (VTC Spring)*, May 2016, pp. 1–6.

[32] R. Weibel and R. J. Hansman, "Safety considerations for operation of different classes of UAVs in the nas," in *AIAA 4th Aviation Technology, Integration and Operations (ATIO) Forum*, p. 6244.

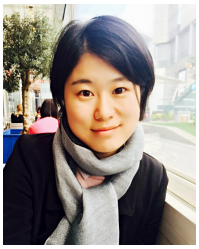

Yongxu Zhu (S'16-M'19) is research associate at Loughborough University now. She received the M.S. degree from the Beijing University of Posts and Telecommunications and Dublin City University, in 2012 and 2013, and the Ph.D degree in Electrical Engineering from University College London in 2017. Her research interests include UAV Communications, wireless edge caching, millimeter-wave communications, heterogeneous cellular networks and physical-layer security.

Gan Zheng (S'05-M'09-SM'12) received the BEng and the MEng from Tianjin University, Tianjin, China, in 2002 and 2004, respectively, both in Electronic and Information Engineering, and the PhD degree in Electrical and Electronic Engineering from The University of Hong Kong in 2008. He is currently Reader of Signal Processing for Wireless Communications in the Wolfson School of Mechanical, Electrical and Manufacturing Engineering, Loughborough University, UK. His research interests include machine learning for communications, UAV communications, edge caching, full-duplex radio, and wireless power transfer. He is the first recipient for the 2013 IEEE Signal Processing Letters Best Paper Award, and he also received the 2015 GLOBECOM Best Paper Award, and the 2018 IEEE Technical Committee on Green Communications & Computing Best Paper Award. He currently serves as an Associate Editor for IEEE Communications Letters.

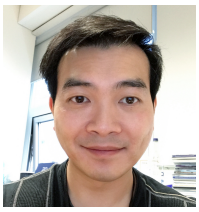

Kai-Kit Wong (M'01-SM'08-F'16) received the BEng, the MPhil, and the PhD degrees, all in Electrical and Electronic Engineering, from the Hong Kong University of Science and Technology, Hong Kong, in 1996, 1998, and 2001, respectively. After graduation, he took up academic and research positions at the University of Hong Kong, Lucent Technologies, Bell-Labs, Holmdel, the Smart Antennas Research Group of Stanford University, and the University of Hull, UK. He is Chair in Wireless Communications at the Department of Electronic and Electrical Engineering, University College London, UK.

He is Fellow of IEEE and IET and is also on the editorial board of several international journals. He has served as Senior Editor for IEEE Wireless Communications Letters since 2016. He had also previously served as Senior Editor for IEEE Communications Letters from 2012 to 2019, Associate Editor for IEEE Signal Processing Letters from 2009 to 2012 and Editor for IEEE Transactions on Wireless Communications from 2005 to 2011. He was also Guest Editor for IEEE JSAC SI on virtual MIMO in 2013 and Guest Editor for IEEE JSAC SI on physical layer security for 5G in 2017.